A Thin-Film Heat Flux Sensor Fabricated on Copper for Heat Transfer Measurements in Parallel Channel Heat Sinks

ICOMM/4M 2010
No. 73

Benjamin A. Jasperson[1], Frank E. Pfefferkorn[2], Weilin Qu[3], Kevin T. Turner[4]

[1]Benjamin A. Jasperson; Mechanical Engr., Univ. of Wisconsin-Madison, USA; bajasperson@wisc.edu

[2]Frank E. Pfefferkorn; Mechanical Engr., Univ. of Wisconsin-Madison, USA; pfefferk@engr.wisc.edu

[3]Weilin Qu; Mechanical Engr., Univ. of Hawaii-Manoa, USA; qu@hawaii.edu

[4]Kevin T. Turner; Mechanical Engr., Univ. of Wisconsin-Madison, USA; kturner@engr.wisc.edu•

ABSTRACT

A combination of lithography-based microfabrication and micro end milling is used to manufacture thin-film resistance temperature detector heat flux sensors on bulk copper substrates. The fabrication process uses photoresist patterning, metal deposition, and lift-off to build the sensor and micro end milling to segment the devices. Micro end milling tests were performed to determine conditions for sensor removal that minimized delamination and burr formation. It was determined that starting on the backside (opposite the sensor) of the copper wafer and machining through to the thin film layers resulted in the least amount of burr formation.

INTRODUCTION

Heat flux is the amount of thermal energy per time transferred through a given area [1]. Heat flux sensors typically rely on one of three operation modes: the gradient method, the transient method, or the active heating method [2]. In most applications, the sensor must be in direct physical and thermal contact with the surface at which the measurement is desired. In large-scale systems, such as nozzle guide vanes of gas turbines, heat flux sensors are often adhered onto the surface [3, 4]. Other applications in which sensors have been directly affixed to the surface include high enthalpy plasma wind tunnel facilities [5] and supersonic wind tunnels [6].

In general, it is desirable to minimize the overall size of heat flux sensors, as it decreases the thermal resistance. This, in turn, minimizes the impact of the sensor on thermal gradients across the device [6]. One application where sensor minimization is beneficial is in the study and design of microscale heat sinks. Heat sinks with features on the scale of hundreds of microns are becoming more prevalent [7-10]. The advancement in heat sink fabrication techniques permits the exploration of numerous designs, including straight channels [7-10] and micro-pin-fins [11-19]. The ability to characterize the heat transfer out of these new devices is vital to the optimization of heat sink design. For such characterization studies, microscale heat flux sensors are needed to measure local heat transfer phenomena.

The microscale heat flux sensors necessary in these situations will require combined manufacturing techniques to facilitate integrated device fabrication on a miniature scale. These techniques will need to embrace fabrication on traditional heat sink materials, such as copper, which are utilized for their high thermal conductivity. In regards to heat flux sensors, lithographic methods are well suited for sensor fabrication on this scale. Likewise, micro end milling is a material removal process capable of machining polymers, metals, ceramics and other materials in three dimensions down to the tens of microns [20].

As such, the goal of this work is to explore the possibility of combining lithography-based sensor fabrication on copper substrates with micro end milling, to produce integrated sensors on micro-scaled devices. The ability to fabricate a heat flux sensor on a copper substrate using lithographic means must be shown. Successful device removal using micro end milling requires that damage to the sensor surface (including delamination and burr formation) be minimized.

PREVIOUS WORK

Heat Flux Sensors

The numerous applications for heat flux sensors means that their performance has been well documented. As such, an exhaustive review of the field is not considered here; the reader is directed towards [21] and [22] for an extensive review.

As previously stated, heat flux sensors typically take one of three configurations: the gradient method, the transient method, or the active heating method [2]. In the gradient method [22, 23], a change in temperature across an intermediate layer is measured and correlated to heat flux, using Fourier's Law. The transient method takes the temperature history at the surface or known location with respect to the

• corresponding author

substrate surface and converts it to heat flux using an inverse heat transfer solution to the problem [3, 21]. In active heating methods, the power required to keep a surface at a specified temperature is monitored [24]. The gradient method was chosen for the device application in the present study due to its potentially fast response time and the requirement of an *in situ* measurement with minimal effects on device thermal gradients.

Machining of laminated structures

Relevant work in composite drilling [25], composite milling [26], and printed circuit board drilling [27] has been performed which can shed light on the challenges of milling layered devices fabricated by lithography. Of particular interest to this study is minimizing delamination. In composite drilling, a critical thrust force is reached where delamination occurs, most often near the exit plane of the material [25]. A sacrificial peel-off ply can be applied to the sensor side of the substrate during machining. The ply may delaminate, but it provides additional thickness and support such that the composite (or sensor, in this case) will not delaminate.

The effects of feed and speed, as well as 2-flute versus 6-flute tools, in composite milling was explored by Davim and Reis [26]. The authors milled channels 2 mm deep using 6 mm diameter tools in a composite material made of carbon fiber reinforced plastics (CFRP). The authors determined that surface roughness and delamination damage were improved using 2-flute tools instead of 6-flute tools. A strong correlation was also observed between increasing feed rate and increasing surface roughness/ delamination.

Lithography on Alternative Substrates

Micro sensors can be fabricated on one substrate (e.g., silicon), removed and glued to the final device [3, 4] or fabricated directly on the material and component of interest [6, 28, 29]. In the latter case, unless the substrate being used for sensor fabrication is shaped prior to lithographic processing, some form of post-lithography machining will be necessary.

Lithographic-based fabrication on non-silicon substrates has been used previously in sensor fabrication [6, 29-32]. In [6], a layered heat flux gage was fabricated directly on a polished 6.25 mm thick aluminum nitride substrate. In [30], strain-gages were fabricated on both polished nickel-based superalloy substrates as well as three-dimensional turbine blades through sputtering techniques. Bhatt et al [32] deposited and fabricated thin film thermocouples on alumina substrates. LIGA has been performed on non-silicon substrates for many years [29, 31].

To the author's knowledge, the combination of heat flux sensor fabrication using lithographic methods on copper, in conjunction with micro end milling for final device production presented here, has not been demonstrated previously. This combination of fabrication techniques allows for novel devices that would be difficult to fabricate on these size scales using other means.

SENSOR DESIGN

The gradient method requires that a temperature difference be measured across a material of known properties in order to measure heat flux. It is based on Fourier's Law:

$$q'' = \frac{k}{d}\left(T_2 - T_1\right) \tag{1}$$

where q'' is heat flux, k is the thermal conductivity of the material, and d is the distance between temperature measurements T_2 and T_1.

In the present study, a resistance temperature detector (RTD) was used for the temperature measurement (Figure 1). The RTD temperature sensor is based on the known temperature/electrical resistance relationship for a given material – namely, as the temperature of a metal increases, the electrical resistance of the metal will also increase [21]. Nickel is used in the current work as it is a cost effective choice (compared to platinum) and the relationship between resistance and temperature is nearly linear over the range of interest.

The relationship for the electrical resistance as a function of temperature in the RTD sensor is:

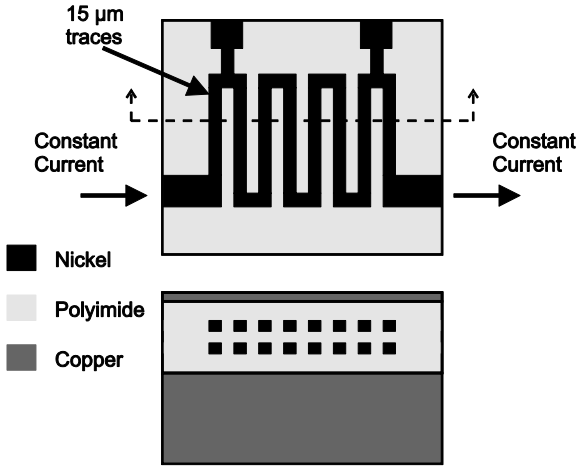

Figure 1: Heat flux sensor

$$R = R_0\left(1 + \alpha\left(T - T_0\right)\right) \quad (2)$$

where R is the resistance of the sensor, R_0 is the initial resistance at reference temperature T_0, and α is the temperature coefficient of the material being used. Experimentally, a constant current is supplied to the sensor and the subsequent output voltage is measured to determine the resistance. Two RTD sensors separated by an electrically and thermally insulating layer (e.g., polyimide) are used to form a heat flux sensor.

The design considerations for heat flux sensors of this type have been addressed in the literature [22, 28]. Of major importance is the sensitivity of the measurement (both temperature and heat flux), self-heating within the sensor, and the thermal resistance imposed on the surface to be measured.

The sensitivity of the overall sensor is composed of the temperature sensitivity (a function of the initial resistance and material properties of the sensor) and the heat flux sensitivity (a function of the thickness between RTD temperature measurements and the conductivity of the insulating material). As outlined in [22], the temperature sensitivity is given as:

$$S_R = \frac{\partial R}{\partial T} = \alpha R_o \quad . \quad (3)$$

Limitations exist on the initial resistance due to ohmic heating from the supplied current. It is desirable to keep the power dissipated to a fraction of the heat flux values being measured [33].

Although increased heat flux sensitivity can be realized through an increase in the thickness between temperature measurements (i.e., increasing the temperature difference for a given heat flux), this will result in increased thermal resistance on the surface being measured. Thus, a balance must be obtained between sensor sensitivity and its impact on the temperature field it is trying to measure.

Calibration of the RTD heat flux sensor requires the determination of two distinct parameters. The initial calibration requires the determination of the resistance/temperature curve for each individual sensor. This can be accomplished using a temperature controlled bath [22]. Increasing the temperature step-wise and acquiring voltage signals from the sensor, a resistance-temperature curve is obtained for each sensor.

Since the thermal conductivity of the insulating layer cannot easily and accurately be measured, an additional calibration step must be performed to determine the combined *k/d* value. This can be done using convective [34], conductive [35], or radiative [5] means of delivering known heat fluxes. In the near future, the parallel heat flux sensor presented here will be calibrated for resistance/temperature curves, heat flux parameters, and transient response.

DEVICE FABRICATION

The bulk device geometry in the current study is approximately 1.5 mm in thickness, 10 mm in width (including contact pads for electrical signals), and 40 mm in length. Each heat flux sensor (four per device) has a footprint of 200 μm by 400 μm, with 15 μm wide traces. Since the final device application will be on a copper heat sink, a copper wafer was chosen as the substrate to facilitate final device fabrication using micro end milling. This allows the sensor to have a minimal thermal impact on the bulk copper heat sink and utilizes the excellent thermal conductivity of copper.

Sensor fabrication consisted of three main tasks: substrate preparation, sensor fabrication (spin coating, lithography and metal deposition), and sensor segmentation (micro end milling).

Substrate Preparation

In order to directly fabricate lithographic sensors, a flat and smooth substrate was required. Since lithographic-based microfabrication processes are tailored for silicon wafers, a three inch wide, 2 mm thick circular copper (alloy 110) wafer was fabricated. This wafer was machined out of bulk copper stock on a vertical CNC mill. The wafer was then bonded to an aluminum puck using Crystalbond® adhesive and mechanically polished. The starting copper was purchased with a "mirror-like" finish and subsequently polished after the wafers were cut. The wafers were initially polished using 6 μm diamond paste on a Velpol polishing cloth from Lapmaster®. This was followed by a similar step using 3 μm diamond paste/Velpol cloth. An arithmetic mean roughness (R_a) of 0.02 μm was achieved through this process. The substrate roughness was characterized using a Zygo white-light interferometer, using a 2.5x objective (trimmed to 2.81 mm by 2.81 mm).

Sensor Fabrication

The device fabrication process is illustrated in Figure 2. The polished wafer (a) was cleaned using (b) an ion milling system, leaving a fresh copper surface for deposition. Without breaking the vacuum in the evaporator chamber, a 7 nm thick chrome layer was deposited, at 0.5 Å/s. The combination of the ion milling and the chrome adhesion layer provided adequate adhesion between the copper wafer and the subsequent sensor layers, as tested qualitatively through peel tests and machining tests. Polyimide 2556 from HD MicroSystems™ was chosen as the insulating material between RTD sensors. A polyimide layer (c) was spun onto the wafer surface, soft baked (120°C for 30 seconds followed by 150°C for 30 seconds) and cured in nitrogen (4°C/min ramp to 200°C, hold for 30 minutes, 2.5°C/min ramp to 300°C, hold for 60 minutes, gradual cooling). A special wafer chuck was used, with additional mechanical support around the perimeter of the wafer, to facilitate spin coating.

A lift-off process was used to fabricate the RTD sensor. The lithographic steps are outlined in parts (d) through (f) of Figure 2. Shipley 1813 positive photoresist was first spun on the copper wafer (d) at 500 RPM for 10 seconds, followed by 30 seconds at 4000 RPM. A soft bake at 120°C for 3 minutes was performed. The soft bake temperature and time were determined by comparing the surface temperature heating and cooling curves for a standard silicon wafer versus the 2 mm thick copper wafers (Figure 3). A thermocouple was adhered to a silicon wafer and a copper wafer, and heating/cooling cycles were compared. The bake temperature and time were tailored to match the time at maximum temperature on the surface of the silicon wafer. This was critical, since the copper wafer had significantly more thermal mass than a standard silicon wafer.

Exposure of the photoresist was performed using a Karl Suss MA6/BA6 contact aligner, 365 nm light at 10 mW. Subsequent development in MF-321 developing solution for 35-45 seconds provided the final step in feature patterning.

Metal deposition for lift-off (e) was performed using an e-beam evaporator. The deposition consisted of a 7 nm thick chrome adhesion layer, followed by a 193 nm nickel layer. After deposition, lift-off (f) of the metal layers was performed using an acetone bath and ultrasonic agitation.

After lift-off, steps (c) through (f) were repeated, completing fabrication of the second RTD

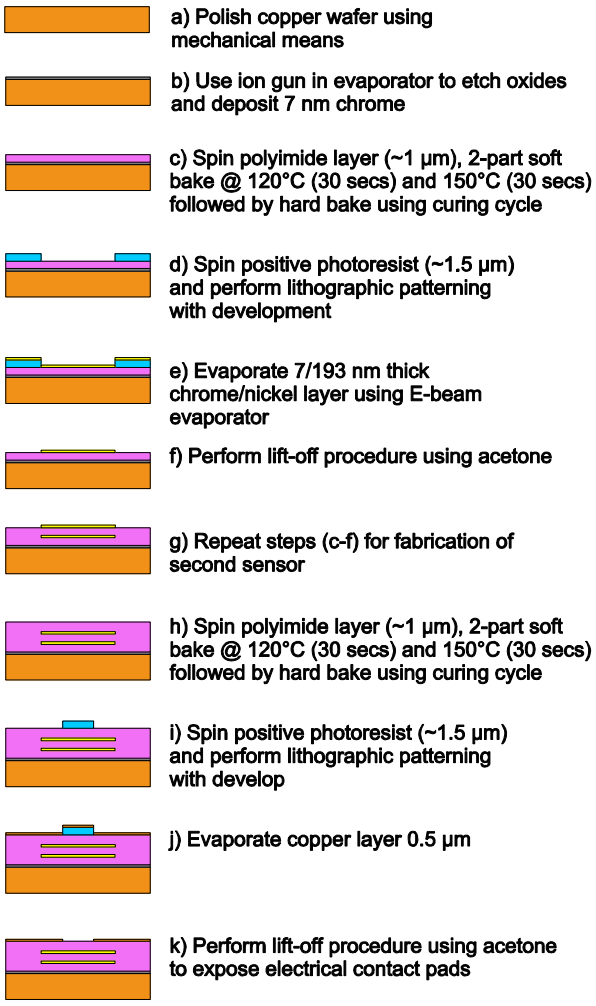

Figure 2: Sensor fabrication steps

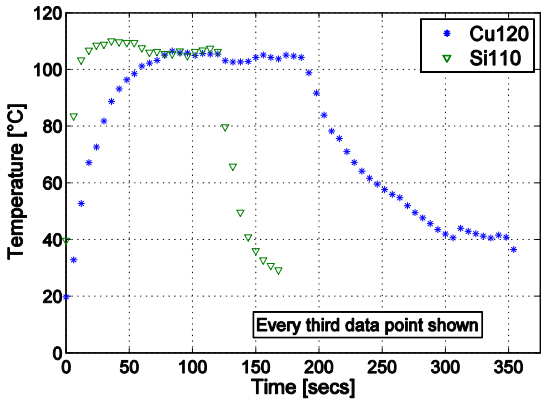

Figure 3: Heating and cooling curves for a 2 mm thick, 3" diameter copper wafer (120°C, 3 minutes) and a 0.381 mm thick, 3" diameter silicon wafer (110°C, 2 minutes)

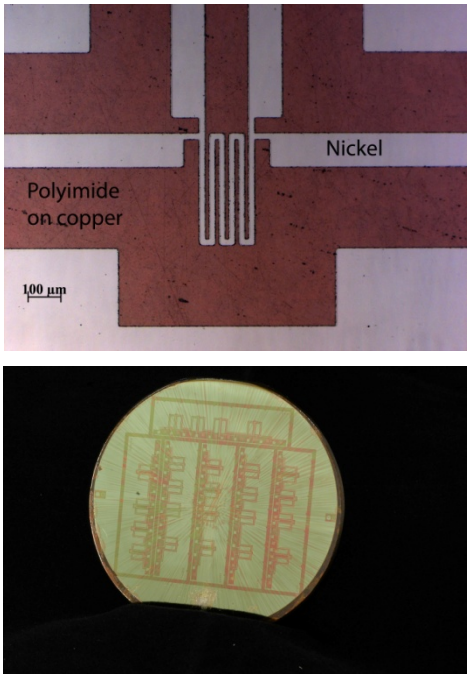

Figure 4: Parallel heat flux sensors
(a) Two RTD temperature sensors on copper (b) Completed 3" wafer with parallel heat flux sensors (prior to copper deposition)

temperature sensor. An optical micrograph of the resulting RTD sensor on copper is shown in Figure 4. The lighter regions are the nickel traces, while the darker regions are the polyimide layers. The small dark spots appearing in the polyimide layers are the result of substrate imperfections. Great care must be taken to obtain a substrate which is as smooth and flat as possible with minimal defects.

An insulating polyimide layer was spun and cured (h) to electrically isolate the second RTD sensor from surrounding media (*e.g,* water). In order to mimic the actual heat sink surface, a copper coating was evaporated on the sensor. Prior to this deposition, photoresist was patterned for lift-off of the electrical contact pads (i-k). The metal contact pads were exposed by etching the polyimide using an O_2 plasma. The copper coating serves as a mask during the plasma etching.

Sensor Segmentation

Following sensor fabrication, individual sensors must be segmented from the wafer. Device segmentation was performed on a HAAS CNC vertical milling machine with a high speed spindle (NSK, HES500). Tests were performed to determine the effects of end milling on the thin lithographic layers. End milling is being investigated because the standard wafer dicing saws are not designed for thicker metal substrates and cannot cut complex 2D paths that are required for some devices.

DELAMINATION STUDIES

To establish a process for cutting the sensor from the wafer with minimal damage to the sensor layers, a machining study was performed. In the machining study, the feed rate and spindle speed (which determines the chip load, defined as the maximum radial depth of cut per flute) were systematically varied. A copper wafer was polished, spin-coated with PI-2556, and cured using the same process as the heat flux sensor. The wafer was secured using step blocks and clamps to a set of parallels that were laid flat on the milling table. The initial study utilized the 1000 µm diameter straight flute micro end mill shown in Figure 5. The goal of the straight flute tool was to minimize any delamination caused by the helix angle. Machining was done on a CNC mill (HAAS TM-1) with a high speed spindle (NSK HES500). The feed rate was varied between 200; 300; and 400 mm/min, while the spindle speed was varied between 10,000; 20,000; and 30,000 RPM. A full-width channel with a depth of cut of 0.5 mm was

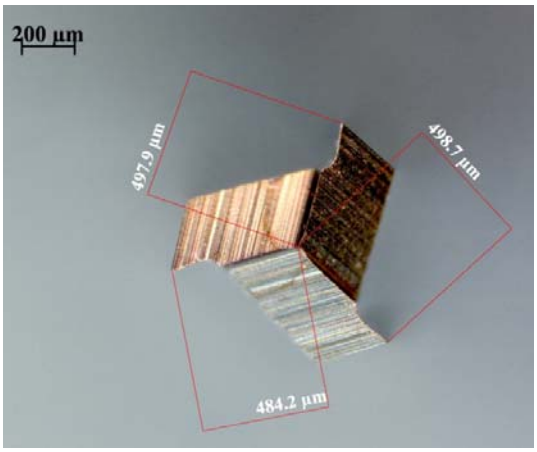

Figure 5: End view of a straight flute micro end mill tool

performed using a water-based cutting fluid (Kool Mist® 78).

The results are summarized through the select images shown in Figure 6. Although feed rate and spindle speed were the factors being varied, chipload appeared to be a better descriptor of the performance. Chipload is calculated from the following equation:

$$C = \frac{F}{N * S} \qquad (4)$$

where C is the chipload [mm/flute], F is the feed rate [mm/min], S is the spindle speed [rev/min], and N is the number of flutes on the tool [flutes/rev].

The results of the machining tests were difficult to quantify due to the non-uniform burr formation along the channel edge. As seen in Figure 6, burr formation along the edge tends to worsen with increasing chipload. Subsequent passes with the end mill cutter were unsuccessful in removing the remaining burrs. A similar set of tests were performed using a 2-flute, 1000 µm diameter end mill with a 30 degree helix. The results showed similar burr formation to those from the straight flute tool.

In an attempt to quantify the damaged area for design

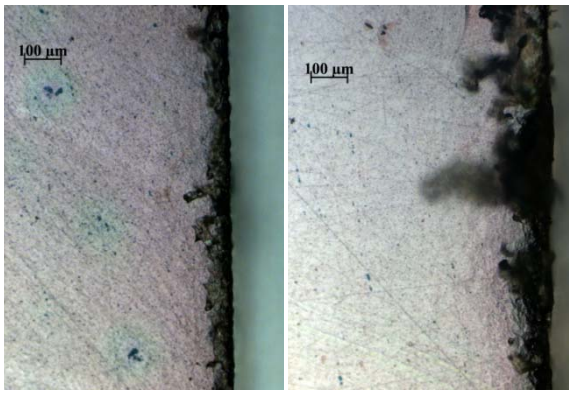

Figure 6: Effect of chipload on edge formation (a) 2 µm chipload (b) 10 µm chipload

purposes, the edges of the channels were cleaned using a cotton swab with water. The damage zone, defined as the longest distance from the channel wall to the unaffected copper surface, was measured using an upright microscope. In general, the damage zone increases with increasing chipload, from 25 µm to 150 µm. Due to the non-uniformity of the damage, conclusive results correlating the effects of chipload, feed, and speed on substrate damage could not be obtained.

Additional tests were performed with constant chipload (5 µm) and increasing spindle speed (10,000; 20,000; 30,000; and 40,000 RPM). The results showed no apparent differences between the runs. Subsequent tests for half-channel cuts (offset = 0.5 mm) for both conventional and climb milling proved to have similar results – no major improvements were observed.

The wafer was then mounted upside down in a vice and machined from the backside, with 0.5 mm axial depth-of-cut, 20,000 RPM spindle speed and 200 mm/min feed rate. The cut was repeated with incremental depth until the channel was machined completely through the wafer. The results show significantly reduced burr formation (see Figure 7). The largest damage zone and burrs formed using this process were approximately 25 µm, as opposed to the 100 µm burrs seen in other tests. These results are encouraging, since backside machining is a critical component in the combined lithographic and micro end milling fabrication. After machining of the wafer to the final overall geometry in future sensors, the devices can be completely removed through backside milling.

CONCLUSIONS

This work has shown the ability to fabricate combined lithographic/micro end milled sensors. Heat flux sensors have been fabricated using lift-off processes on a copper wafer. In addition, representative structures with reasonable delamination have been machined using micro end milling.

ACKNOWLEDGEMENTS

This work was supported by National Science

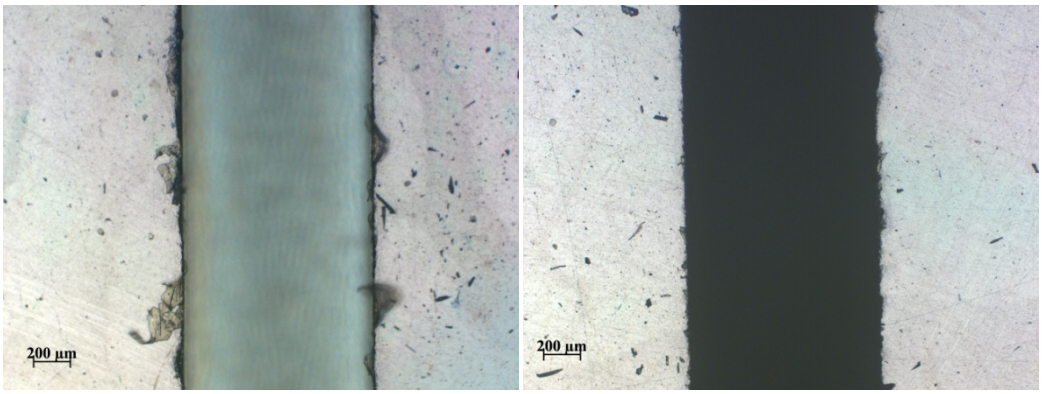

Figure 7: Peeling of polyimide post machining, 20,000 [RPM], feed = 200 mm/min, for (a) sensor-side machining and (b) back-side machining

Foundation grants CBET-0729693 (University of Wisconsin-Madison) and CBET-0730315 (University of Hawai'i at Manoa).

NOMENCLATURE

q''	*heat flux [W/m^2]*
k	*conductivity [W/m-K]*
d	*distance between sensors [m]*
T_1	*RTD1 temperature [K]*
T_2	*RTD2 temperature [K]*
R	*Electrical resistance [Ω]*
R_0	*Nominal electrical resistance @T_0 [Ω]*
α	*Temperature coefficient [1/K]*
T	*Measured temperature [K]*
T_0	*Nominal temperature [K]*
S_R	*Sensitivity, temperature [Ω/K]*
C	*Chipload [mm]*
F	*Feed rate [mm/min]*
S	*Spindle speed [rev/min]*
N	*# of flutes per tool [flute/rev]*

REFERENCES

[1] J. G. Webster, "The measurement, instrumentation, and sensors handbook," CRC Press LLC, 1999.

[2] J. Chun, S. H. Oh, S. S. Lee, and K. Moohwan, "Design and fabrication of micro heat flux sensor," in *Proceedings of the 1999 IEEE/RSJ International Conference on Intelligent Robots and Systems Conference*, 1999, pp. 1045-1048.

[3] S. M. Guo, C. C. Lai, T. V. Jones, M. L. G. Oldfield, G. D. Lock, and A. J. Rawlinson, "The application of thin-film technology to measure turbine-vane heat transfer and effectiveness in a film-cooled, engine-simulated environment," *International Journal of Heat and Fluid Flow,* vol. 19, no. 6, 1998, pp. 594-600.

[4] E. Piccini, S. M. Guo, and T. V. Jones, "The development of a new direct-heat-flux gauge for heat-transfer facilities," *Measurement Science and Technology,* vol. 11, no. 4, 2000, pp. 342-349.

[5] S. Lohle, J. Battaglia, J. Batsale, O. Enouf, J. Dubard, and J. Filtz, "Characterization of a heat flux sensor using short pulse laser calibration," *Review of Scientific Instruments,* vol. 78, no. 5, 2007, pp. 53501.

[6] J. M. Hager, and L. W. Langley, "Microsensors for high heat flux measurements," *Journal of thermophysics and heat transfer,* vol. 7, no. 3, 1993, pp. 531-534.

[7] K. Kawano, K. Minakami, H. Iwasaki, and M. Ishizuka, "Micro channel heat exchanger for cooling electrical equipment," in *Proceedings of the 1998 ASME International Mechanical Engineering Congress and Exposition Conference*, 1998, pp. 173-180.

[8] P.-S. Lee, S. V. Garimella, and D. Liu, "Investigation of heat transfer in rectangular microchannels," *International Journal of Heat and Mass Transfer,* vol. 48, no. 9, 2005, pp. 1688-1704.

[9] W. Qu, and I. Mudawar, "Experimental and numerical study of pressure drop and heat transfer in a single-phase micro-channel heat sink," *International Journal of Heat and Mass Transfer,* vol. 45, no. 12, 2002, pp. 2549-2565.

[10] D. B. Tuckerman, and R. F. W. Pease, "High-performance heat sinking for VLSI," *IEEE Electronic Devices Letters,* vol. EDL-2, no. 5, May 1981, pp. 126-129.

[11] A. Kosar, C.-J. Kuo, and Y. Peles, "Hydroil-based micro pin fin heat sink," in *Proceedings of the 2006 ASME International Mechanical Engineering Congress and Exposition Conference*, 2006.

[12] A. Kosar, C. Mishra, and Y. Peles, "Laminar flow across a bank of low aspect ratio micro pin fins," *Journal of Fluids Engineering, Transactions of the ASME,* vol. 127, no. 3, 2005, pp. 419-430.

[13] A. Kosar, and Y. Peles, "Thermal-hydraulic performance of MEMS-based pin fin heat sink," *Journal of Heat Transfer,* vol. 128, no. 2, 2006, pp. 121-131.

[14] Y. Peles, and A. Kosar, "Convective flow of refrigerant (R-123) across a bank of micro pin fins," *International Journal of Heat and Mass Transfer,* vol. 49, no. 17-18, 2006, pp. 3142-3155.

[15] Y. Peles, A. Kosar, C. Mishra, C.-J. Kuo, and B. Schneider, "Forced convective heat transfer across a pin fin micro heat sink," *International Journal of Heat and Mass Transfer,* vol. 48, no. 17, 2005, pp. 3615-3627.

[16] R. S. Prasher, J. Dirner, J.-Y. Chang, A. Myers, D. Chau, D. He, and S. Prstic, "Nusselt number and friction factor of staggered arrays of low aspect ratio micropin-fins under cross flow for water as fluid," *Journal of Heat Transfer,* vol. 129, no. 2, 2007, pp. 141-153.

[17] W. Qu, and A. Siu Ho, "Liquid single-phase flow in an array of micro-pin-fins. Part I. Heat transfer characteristics," *Journal of Heat Transfer,* vol. 130, no. 12, 2008, pp. 122402 (122411 pp.).

[18] W. Qu, and A. Siu Ho, "Liquid single-phase flow in an array of micro-pin-fins. Part II: pressure drop characteristics," *Journal of Heat Transfer,* vol. 130, no. 12, 2008, pp. 124501 (124504 pp.).

[19] A. Siu-Ho, W. Qu, and F. Pfefferkorn, "Experimental study of pressure drop and heat transfer in a single-phase micro-pin-fin heat sink," *Transactions of the ASME. Journal of Electronic Packaging,* vol. 129, no. 4, 2007, pp. 479-487.

[20] D. L. Wissmiller, and F. E. Pfefferkorn, "Technical paper: Micro end mill tool temperature measurement and prediction," *Journal of Manufacturing Processes,* vol. 11, no. 1, 2009, pp. 45-53.

[21] T. E. Diller, "Advances in Heat Flux Measurements," *Advances in Heat Transfer*, pp. 279-353, 1993.

[22] H. Mocikat, and H. Herwig, "Heat Transfer Measurements with Surface Mounted Foil-Sensors in an Active Mode: A Comprehensive Review and a New Design," *Sensors,* vol. 9, no. 4, 2009, pp. 3011-3032.

[23] H. Mocikat, and H. Herwig, "Heat transfer measurements in fully turbulent flows: Basic investigations with an advanced thin foil triple sensor," *Heat and Mass Transfer/Waerme- und Stoffuebertragung,* vol. 44, no. 9, 2008, pp. 1107-1116.

[24] D. S. Campbell, M. Gundappa, and T. E. Diller, "Design and calibration of a local heat-flux measurement system for unsteady flows," *Journal of Heat Transfer,* vol. 111, no. 2, 1989, pp. 552-557.

[25] S. Jain, and D. C. H. Yang, "Effects of feedrate and chisel edge on delamination in composites drilling," *Journal of engineering for industry,* vol. 115, no. 4, 1993, pp. 398-405.

[26] J. P. Davim, and P. Reis, "Damage and dimensional precision on milling carbon fiber-reinforced plastics using design experiments," *Journal of Materials Processing Technology,* vol. 160, no. 2, 2005, pp. 160-167.

[27] B. K. Hinds, and M. Treanor, "Drilling of printed circuit boards: factors limiting the use of smaller drill sizes," *Proceedings of the Institution of Mechanical Engineers Part B-Journal of Engineering Manufacture,* vol. 214, no. 1, 2000, pp. 35-45.

[28] J. M. Hager, S. Onishi, L. W. Langley, and T. E. Diller, "Heat flux microsensors," in *Proceedings of the Conference*, 1989, pp. 1-8.

[29] S. K. Griffiths, M. W. Losey, J. T. Hachman, D. M. Skala, L. L. Hunter, N. Y. C. Yang, D. R. Boehme, J. S. Korellis, G. Aigeldinger, W. Y. Lu, L. J. Kelly, M. A. Hekmaty, D. E. McLean, P. C. Y. Yang, C. A. Hauck, and T. A. Friedmann, "Resist substrate studies for LIGA microfabrication with application to a new anodized aluminum substrate," *Journal of Micromechanics and Microengineering,* vol. 15, no. 9, 2005, pp. 1700-1712.

[30] P. Kayser, J. C. Godefroy, and L. Leca, "High-Temperature Thin-Film Strain-Gauges," *Sensors and Actuators a-Physical,* vol. 37-8, 1993, pp. 328-332.

[31] W. Ehrfeld, P. Bley, F. Gotz, J. Mohr, D. Munchmeyer, W. Schelb, H. J. Baving, and D. Beets, "Progress in deep-etch synchrotron radiation lithography," in *Proceedings of the 31st International Symposium on Electron, Ion, and Photon Beams Conference*, 1988, pp. 178-182.

[32] H. D. Bhatt, R. Vedula, S. B. Desu, and G. C. Fralick, "Thin film TiC/TaC thermocouples," *Thin Solid Films,* vol. 342, no. 1, 1999, pp. 214-220.

[33] A. H. Epstein, G. R. Guenette, R. J. G. Norton, and Y. Cao, "High-frequency response heat-flux gauge," *Review of Scientific Instruments,* vol. 57, no. 4, 1986, pp. 639-649.

[34] G. J. Borell, and T. E. Diller, "A convection calibration method for local heat flux gages," *Transactions of the ASME. Journal of Heat Transfer,* vol. 109, no. 1, 1987, pp. 83-89.

[35] M. Rencz, E. Kollar, and V. Szekely, "Heat-flux sensor to support transient thermal characterization of IC packages," *Sensors and Actuators A (Physical),* vol. A116, no. 2, 2004, pp. 284-292.